AEGC2019 Data to Discovery
Australasian Exploration Geoscience Conference
2-5 September 2019 • Perth, Western Australia
Incorporating the AIG, ASEG, PESA, and WABS

Computing the head wave coefficient with multi-fold near-surface seismic refraction data

Derecke Palmer
The University of New South Wales
Sydney 2052 Australia
d.palmer@unsw.edu.au

SUMMARY

Head wave amplitudes are dominated by an extremely rapid decrease with increasing source-to-receiver separation. Nevertheless, the standard corrections for geometric spreading are usually quite adequate and are not critical with multi-fold reversed refraction data.

The head wave coefficients (HWC), which are the refraction analogue of the reflection coefficients, are essentially equivalent at coincident sources and receivers. It supports a 2D revision of the standard 1D head wave expression.

HWCs can be readily computed with a variety of methods using both the measured head wave amplitudes and full waveform refraction images.

Key words: refraction, amplitudes, head wave coefficient, full waveform imaging.

AMPLITUDE – UNDERVALUED & NEGLECTED

Any search of the literature will reveal numerous studies which describe disparate methods for picking first arrival traveltimes. However, there are very few published studies, which make the simple leap of a quarter of a cycle to investigate the amplitude of the head wave arrival. Whereas the analysis of both amplitudes and traveltimes is integral to the evaluation of reflection data, routine near surface seismic refraction investigations have been stalled at the first breaks for almost a century.

The major objective of this study is to demonstrate that the computation of the head wave coefficient (HWC), the refraction analogue of the reflection coefficient, poses very few difficulties with routine multi-fold near surface seismic refraction data. Consistent and reliable measures of the HWC can be obtained readily with a variety of methods using both the measured head wave amplitudes and full waveform refraction images.

There are two useful benefits with the analysis of the HWC. First, the spatial resolution is significantly better than that which can be achieved with the detailed analysis of traveltimes using the generalised reciprocal method (GRM). Second, the P-wave HWC can be readily inverted to obtain useful measures of the S-wave seismic velocities. It is anticipated that these inverted parameters will be applicable in their own right with routine geotechnical investigations, as well as for generating starting models for full waveform inversion as these methods systematically become realistic, reliable and routine with near surface seismic refraction data.

This study employs the data for a 2 km section of the Wirrinya traverse 99WR-HR1, which was recorded over 17 km of the Palaeozoic Lachlan Fold Belt in south-eastern Australia. This section has been selected because detailed models of the P-wave seismic velocities in the sub-weathered region have been computed previously from the traveltime data with 1.5D and 2D inversion algorithms (Palmer, 2015).

THE 1D MODEL OF THE HEAD WAVE AMPLITUDE

Equation 1 is the standard 1D model of the head wave amplitude for plane homogeneous layers. It includes K, the HWC, F(t), the source function, r, the source-to-receiver distance, and L, the "glide distance".

$$Amplitude = \frac{K\,F(t)}{(r\,L^3)^{1/2}} \qquad (1)$$

The glide distance is the interval that the refracted energy has travelled in the refractor. It can be reasoned that the glide distance is approximately equal to the source-to-receiver distance minus the optimum XY value of the GRM.

The denominator is usually taken as the geometric spreading factor. Equation 2 shows the approximation used in this study.

$$(r\,L^3)^{1/2} \cong (r\,(r-XY)^3)^{1/2} \cong r\,(r-1.5\,XY) \qquad (2)$$

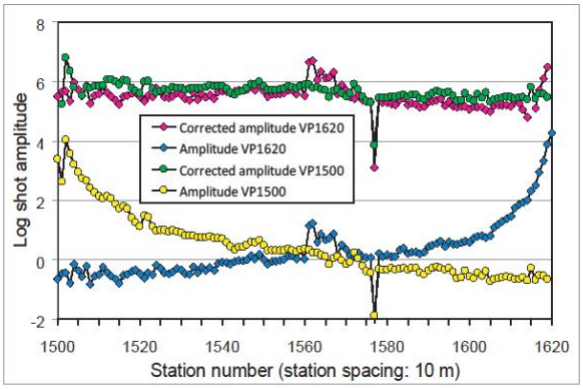

Figure 1: Measured and offset corrected shot amplitudes.

Figure 1 presents the measured head wave amplitudes for two reversed shot records, together with the values corrected for the geometric spreading using the approximation in Equation 2. The geometric correction used is r(r-50), which corresponds with an average optimum XY value of 35 m.

Figure 1 shows that the head wave amplitudes of the Wirrinya data vary by more than four orders of magnitude, or more than 80 dB (20 $log(^{3000}/_{0.3})$), whereas the offset corrected head wave amplitudes generally vary by less than one order of magnitude (12 dB). It is posited that the longstanding neglect of the HWC can be attributed, in part, to its concealment by the very large geometric spreading component.

Figure 1 shows that the forward and reverse offset corrected head wave amplitudes differ. This effect is usually attributed to dipping and/or irregular interfaces. In this study, the forward and reverse head wave amplitudes are multiplied, in order to minimise the effects of dip and any variations in the angle of emergence of the seismic energy (Palmer, 2001a).

COMPOSITING HEAD WAVE AMPLITUDES

Whereas the traveltimes in different sections of the weathered and sub-weathered regions are added to obtain the total traveltime, Equation 1 demonstrates that the individual amplitude components are multiplied. Therefore, all of the processing operations undertaken in this study generally involve a linearization of the computations through the simple process of transforming the amplitudes with logarithms.

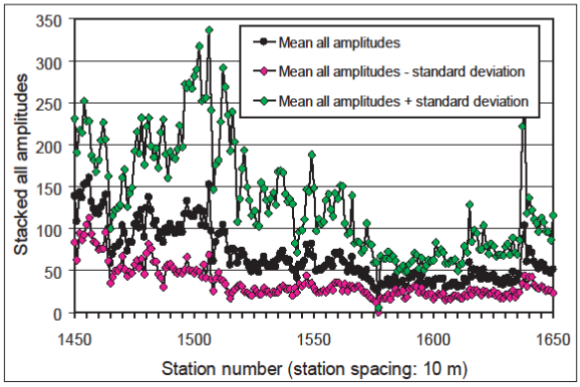

Figure 2: Offset corrected stacked amplitudes.

Figure 2 presents the head wave amplitudes, which have been corrected for offset with Equation 2, for source-to-receiver offsets greater than 200 m, and which have been averaged at each receiver station. The 200 m gap is approximately the cross-over distance, which marks the transition of traveltimes from the weathered region to those from the sub-weathered region (Palmer 2015, Figure 4). In general, there are up to 50 values in the forward and reverse directions at each station, and therefore, up to 100 values in the composited average. Averaging 100 values at each receiver station represents the averaging of the source function over 2000 m.

Since the head wave amplitudes were first transformed with logarithms, the average is a geometric mean. The average standard deviation is a factor of approximately 1.6.

Although not shown here, the offset corrected composited amplitudes differ in the forward and reverse directions, as is also the case with the single shot record values in Figure 1. The geometric mean of the forward and reverse offset corrected amplitudes at each receiver station will be taken as a measure of the unscaled HWC.

THE SOURCE FUNCTION

From Equation 1, it can be seen that a measure of the source function F(t) can be obtained by dividing the offset corrected amplitudes for each common shot gather by the average HWC at each receiver station. The source functions differ in the forward and reverse directions, as is also the case with the stacked offset corrected amplitudes at common receiver gathers. Therefore, an average source function for each shot record has been computed by averaging over all traces with offsets greater than 200 m, which is generally 200 traces (240 traces per shot gather minus a gap of 20 traces for the cross-over distance in each direction).

Figure 3 presents the average HWCs and the averaged source function which has been scaled to correspond with the HWC at the receivers. The correlation coefficient between these two sets of values is 0.906. The standard deviations for the averaged HWCs and the averaged source functions are similar.

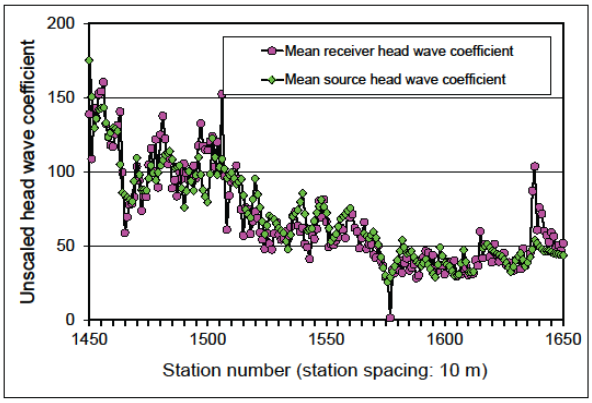

Figure 3: Comparison of the average head wave coefficients and the scaled averaged source functions.

The minor differences between the average HWCs and the scaled averaged source functions can be attributed in part, to a combination of a lateral offset of approximately 5 m between the source and receiver lines, which were located on and alongside existing unsealed rural thoroughfares, together with a 5 m separation between the sources and the nearest receivers along the receiver line. Also, there is a further separation of several metres between the adjacent sources. It indicates that most of the medium and long wavelength variations have a geological origin, rather than represent an expression of any acquisition footprint.

Furthermore, there is a low amplitude "noise envelope" with a short spatial wavelength of approximately 30-50 m superimposed on the receiver head wave coefficient. The low amplitude noise envelope is attributed to very near surface soil variations.

2D MODEL OF THE HEAD WAVE AMPLITUDE

Červený and Ravindra (1971; Equation 3.107) relate the HWC to the product of two separate transmission coefficients. The results in Figure 3 suggest that these two transmission coefficients are equivalent to the source function, which can now be updated to an effective HWC at the source K_{source}, and the HWC at the receiver. In addition, there is an overall scaling factor, which is the product of the strength of the source and the amplification of the recording system, and which can now be

included into an updated source function F(t). Therefore, a revised 2D version of Equation 1 is proposed, namely:

$$Amplitude = \frac{K_{source} K_{receiver}\, F(t)}{(r\, L^3)^{1/2}} \quad (3)$$

Equation 3 has two far reaching implications.

First, Equation 3 emphasises a fundamental difference between refraction and reflection methods. Whereas the up-going and down-going transmission coefficients computed with the Zoeppritz equations are different with reflection signals at the same interface, Figure 3 shows that the corresponding transmission coefficients, now termed the source and receiver HWCs, are the same with refraction signals.

The apparent paradox occurs at the receiver rather than the source. The Zoeppritz equations show that the transmission coefficient is greater than one when the seismic energy propagates from a medium of higher acoustic impedance to one of lower acoustic impedance. However, the approximation of the HWC in equation 4 (Palmer, 2001b, Equation 3), shows that it is generally less than one.

$$K \propto 2\, \frac{\rho_1 \propto_1}{\rho_2 \propto_2} \quad (4)$$

where α is the seismic velocity and ρ is the density.

Second, Equation 3 implies the same reciprocity with head wave amplitudes, as is usually associated with refraction traveltime methods. Therefore, standard refraction traveltime inversion algorithms can be employed, following the correction for geometrical spreading with Equation 2, and the linearization of Equation 3 with logarithms. This study demonstrates that the 1.5D algorithms of the COG GRM, and a combination of the 2D algorithms of the intercept time (ITM) and the common reciprocal methods (CRM) (Palmer, 2009), can generate useful estimates of the HWCs using head wave amplitudes which have been corrected for geometric spreading.

These algorithms are able to accommodate dipping and/or irregular interfaces through the explicit identification of forward and reverse traveltimes within the algorithms. Although not derived explicitly in this study, it will be assumed that these algorithms can also accommodate similar dip effects with the transformed head wave amplitudes.

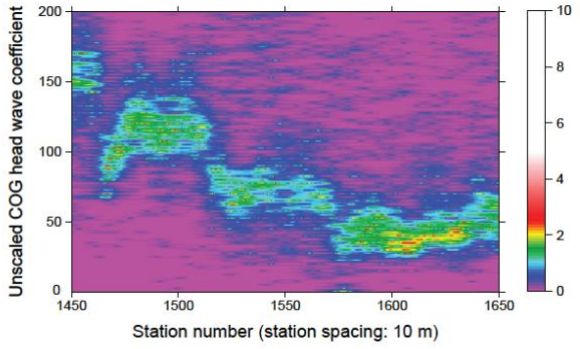

Figure 4: Histogram of COG head wave coefficients.

1.5D COG GRM HEAD WAVE COEFFICIENTS

Figure 4 presents a histogram of the parameter which has been computed with the COG GRM time model algorithm (Palmer, 2013). It essentially represents the unscaled HWC, which is obtained by averaging the logarithms of the forward and reverse offset corrected amplitudes. Furthermore, the subtraction of a term, which corresponds with the averaged reciprocal time with the traveltime equivalents, effectively compensates for the different source functions, because of the reciprocity implied with Equation 3.

2D CRM HEAD WAVE COEFFICIENTS

The common reciprocal method (CRM) algorithm for the computation of a 2D time model explicitly identifies forward and reverse traveltimes, and therefore, it can accommodate dipping and/or irregular interfaces. However, there can be bulk or "static" shifts between overlapping sets of computations with multi-fold data, because of errors in the reciprocal times. Therefore, rather than relying on the precision of a single measurement of the reciprocal time from the shot records, a two-stage process, which computes an average reciprocal time by differencing long and short wavelength time and (and amplitude) models (Palmer, 2009) is used. First, so-called "long wavelength" models are generated at each source location with forward and reverse intercept times. Second, so-called "short wavelength" models are generated at each receiver location using the standard CRM algorithm.

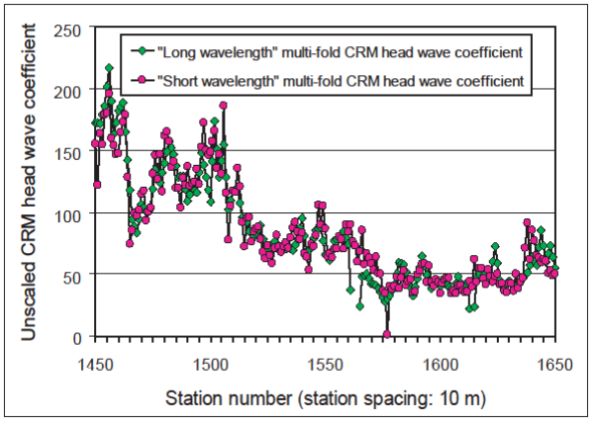

Figure 5: Long and short wavelength CRM derived head wave coefficients.

Figure 5 presents the multi-fold long and short wavelength CRM HWCs.

THE STACKED RCS

The essential process for the generation of the short wavelength time model with the CRM is the addition of the forward and reverse scalar traveltimes. The refraction convolution section (RCS) achieves the equivalent process through the convolution of the corresponding seismic traces, since convolution adds phase, that is, traveltimes, and multiplies amplitudes (Palmer, 2001a). Therefore, the stacked RCS corresponds with the averaged short wavelength time model. However, the stacked RCS constitutes an arithmetic, rather than a geometric average of the amplitude products.

Figure 6 presents the stacked RCS. Fold is generally 40. The amplitudes of the stacked RCS are measured prior to deconvolution and trace balancing. The amplitudes shown in Figure 7 are the square root of the stacked RCS amplitudes, because convolution multiplies the shot amplitudes.

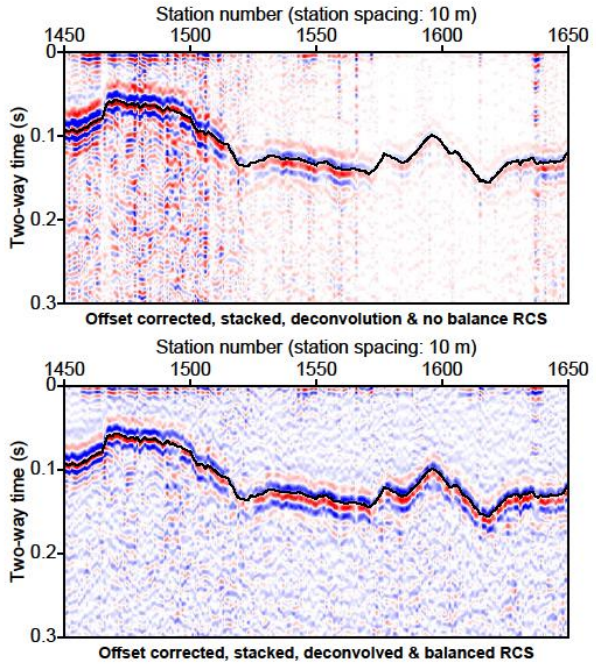

Figure 6: RCS computed before and after amplitude equalisation with trace balancing. The scalar CRM time model is also shown.

The stacked RCS HWCs in Figure 7 shows the same long wavelength amplitude variations as the averaged amplitude products in Figures 2-5. There are four intervals, namely stations 1450-1460, 1460-1525, 1525-1575, and 1575-1650 where the values are generally similar. The up to 40-fold stacking has effectively averaged the various source functions over a distance of up to 1600 m (80 VPs @ 20 m).

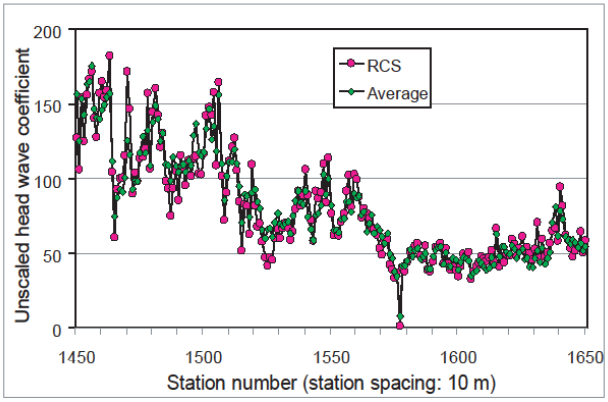

Figure 7: Comparison of the RCS-derived HWCs and average of all amplitude-derived HWCs.

Figure 8 presents a compilation of the unscaled HWCs computed with the various methods described previously.

CONCLUSIONS

The extremely rapid decrease in the head wave amplitude with increasing source-to-receiver distance usually conceals any spatial variations in the head wave coefficient. Nevertheless, simple methods for correcting for the geometrical spreading are usually sufficiently precise with forward and reverse data.

A longstanding failure to adopt simple methods of full waveform imaging of near surface refraction data has not enabled the convenient integration of amplitudes and detailed geological structure within a single presentation.

The amplitudes of the stacked RCS are comparable to the unscaled HWCs computed from the head wave amplitudes obtained from the shot records. It is concluded that the stacked RCS constitutes the most convenient strategy for computing the HWC because it combines the three operations of correcting for geometrical spreading, compensating for the effects of dipping interfaces, and stacking into a single operation. The 40-fold stacking also provides useful improvements in signal-to-noise ratios (20 log√40=16 dB).

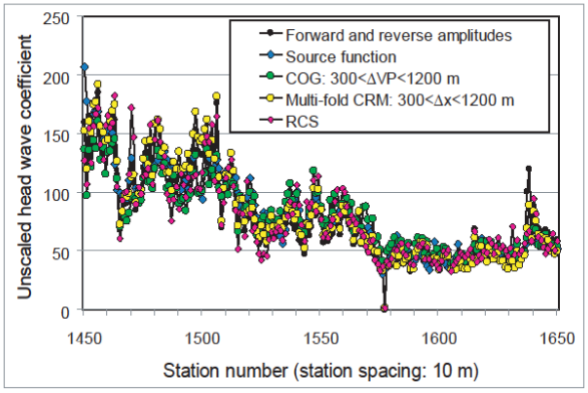

Figure 8: Compilation of all head wave coefficients.

REFERENCES

Červený, V., Ravindra, R., 1971, Theory of seismic head waves, University of Toronto Press, Toronto.

Palmer, D, 2001a, Imaging refractors with the convolution section, *Geophysics* 66, 1582-1589.

Palmer, D, 2001b, Resolving refractor ambiguities with amplitudes, *Geophysics* 66, 1590-1593.

Palmer D. 2009. Integrating short and long wavelength time and amplitude statics. *First Break* 27(6), 57–65.

Palmer, D., 2013, Resolving complex structure in near-surface refraction seismology with common offset gathers: *The Leading Edge*, 32, 680-690.

Palmer, D., 2015, Is accuracy more important than precision in near surface refraction seismology? *Near Surface Geophysics*, 13, 1-18.